Climate Dynamics
https://doi.org/10.1007/s00382-022-06561-1

# North American fire weather catalyzed by the extratropical transition of tropical cyclones

**Jacob Stuivenvolt-Allen**[1,2] · **S.-Y. Simon Wang**[1]

Received: 20 July 2021 / Accepted: 23 October 2022


**Abstract**
When tropical cyclones in the western North Pacific transition into midlatitude cyclones, it often perturbs the jet stream, resulting in amplified flow conditions in the north Pacific and various weather extremes in North America. Thus far, however, the climatological impacts of extratropical transitioning cyclones (ETCs) on North American fire weather are mostly undocumented. In this study, we group ETCs by the characteristics that are important for their interaction with the jet stream and document the response in North American fire weather. We find that ETCs are consistently associated with broad swaths of suppressed fire weather along with smaller areas of enhanced fire weather in North America, mostly through anomalous upper-level circulation and near-surface temperatures. While the chaotic nature of the ETC and jet stream interaction means that ETCs grouped by similar characteristics and locations can result in varying downstream responses, the composite analysis reveals some areas of consistently altered fire weather for ETCs which recurve at certain longitudinal ranges, including the Pacific Northwest and northern Intermountain West. At a time in which the risk and extent of wildfires in the Western United States is an issue of growing concern, this study represents the first holistic understanding of how ETCs' downstream perturbations impact fire weather.

**Keywords** Fire weather · Tropical cyclones · Rossby waves · Compounding extremes · Typhoons

## 1 Introduction

The peak of tropical cyclone activity and associated interactions with the jet stream (Archambault et al. 2013; Balch et al. 2017), from July through October, coincides with peak fire season in western North America. While the actual ignition and ecological precursors for fire (i.e. fuel load, seasonal drought) are mostly independent of the impact of typhoons, fire weather including winds, humidity, and temperature in the western US can be significantly impacted by amplified flow due to upstream typhoons (Bosart et al. 2017; Grams et al. 2013). September of 2020 was a notable example of how the extratropical flow response to tropical cyclones can result in catastrophic fire outbreaks and spread (Stuivenvolt-Allen et al. 2021). Days before the fire outbreak in the Pacific Northwest on the 8th of September, three typhoons made an extratropical transition near the Korean peninsula in quick succession, resulting in a Rossby wave train across the north Pacific. Subsequently, a strengthened pressure gradient formed directly over the Pacific Northwest resulting in record-breaking winds and rapid fire spread throughout the region (Stuivenvolt-Allen et al. 2021). Research has shown that typhoons interacting with the jet stream can result in downstream weather extremes (Bosart et al. 2017), but the relationship between tropical cyclones and fire weather has not been examined holistically. Subsequently, our objective is to create composites of western North Pacific tropical cyclones and their extratropical interaction to examine their relationship with altered fire weather in western North America.

The mechanisms underlying a typhoon and jet stream interaction have been extensively studied. Tropical cyclones which undergo an extratropical transition (ETCs)—defined as a tropical cyclone that travels into the mid-latitudes and re-intensifies as a cold core extratropical cyclone—have potential for causing lasting and energetic flow amplification in the North Pacific, though recurving typhoons which

✉ Jacob Stuivenvolt-Allen
jacob.stuivenvolt-allen@yale.edu

[1] Department of Plants, Soils, and Climate, Utah State University, Logan, UT, USA

[2] Department of Earth and Planetary Sciences, Yale University, New Haven, CT, USA

Published online: 08 November 2022

do not transition can also result in amplified flow patterns (Agustí-Panareda et al. 2005; Archambault et al. 2013; Harr and Dea 2009; Hodyss and Hendricks 2010; Pantillon et al. 2013). As an immense source of diabatic heating, ETCs facilitate the advection of low potential vorticity (PV) into the jet region, resulting in a localized ridge and an intensified jet streak to the north of the ETC (Evans et al. 2017; Grams et al. 2015; Riemer and Jones 2010). This process catalyzes extratropical cyclogenesis adjacent to the jet streak and the associated Rossby wave energy dispersion results in an alternating atmospheric wave train which spans across the entire north Pacific (Archambault et al. 2013, 2015; Orlanski and Sheldon 1995).

The interaction between an ETC and the north Pacific wave guide changes with respect to the seasonality, intensity, and position of an ETC. More specifically, previous research has highlighted that the north Pacific flow in August, September and October is most conducive for amplification due to tropical cyclone-jet interactions (Archambault et al. 2013). From July to October, ETCs become stronger by both measures of central mean sea level pressure (MSLP) and the radius of 30 kt winds at recurvature. The longitudinal position of recurvature is also a critical component for determining the strength of the ETC-extratropical flow interaction, with stronger interactions occurring with ETCs that recurve farther west (Archambault et al. 2013). The large variability of storm characteristics (position, intensity, and seasonality) is one component of the extratropical flow interaction, as the characteristics of the north Pacific flow at the time of recurvature are also important for determining whether the ETC's impact is constructive. Constructive interactions can occur if an ETC becomes phase locked with an approaching trough (meaning the ETC and the trough converge in space and time) and the impact of the ETC is resonant with the existing wave structure. This generally results in more amplified downstream responses (Aiyyer 2015; Grams et al. 2015; Riboldi et al. 2019). Additionally, the intensity and position of the subtropical jet stream impacts the amplitude of the downstream wave response, with more intense jet speeds resulting in greater wave amplification (Finocchio and Doyle 2019). These factors which influence the relationship between a typhoon and amplified flow will be analyzed to determine if enhanced fire weather in North America changes in response to ETC characteristics.

The existing knowledge of ETCs and recurving typhoons highlights that subsequent analysis of the fire weather response to ETCs must account for seasonal variability in the midlatitude flow, along with the spatial and intensity variability of an ETC. Due to the potential for amplified flow to greatly impact fire spread and intensity, we group ETC events into categories that are important for their associated impacts to analyze the response of North American fire weather. ETCs are grouped by seasonality, location, intensity, and the strength of their interaction with the midlatitude flow. Using the Canadian Fire Weather Index, a fire severity rating that depends on fuel moisture and weather conditions (Wagner et al. 1987), we will determine how these different ETC characteristics impact the likelihood of enhanced fire weather.

## 2 Methods

### 2.1 Data

For the record of typhoon position, timing, intensity, and classification, we use the Japanese Meteorological Agency's (JMA) Best Track Dataset which is provided by the Regional Specialized Meteorological Center (https://www.jma.go.jp). While discrepancies have been documented between the Best Track Dataset and observations due to its empirical derived estimates of tropical cyclone intensity, this dataset fits the needs of this study by providing accurate enough data for categorical grouping of tropical cyclones (Archambault et al. 2013, 2015; Barcikowska et al. 2012). The response of the atmosphere to ETCs will be analyzed using the National Center for Environmental Prediction-Department of Energy's Reanalysis 2 (NCEP R2) at daily intervals (Kanamitsu et al. 2002). As the diabatic outflow from a tropical cyclone is prominent in the upper level, we will use daily geopotential height at 200 hPa (z200) to analyze the impact of the ETC on recurvature. We use daily NCEP R2 data to match the format of the FWI described below and because it was more efficient in creating composites. For evaluating the strength of the ETC and jet interaction, we compute potential vorticity advection using the European Centre for Medium-Range Weather Forecasts ERA5 global reanalysis data as the diabatic outflow of an ETC will be better captured with the 0.25° resolution (Hersbach et al. 2020). PV advection is calculated at the closest six-hour interval to T0, a reference time for each ETC described in Sect. 2.3.

To determine the likelihood of fire weather conditions after the recurvature of a western Pacific typhoon, we use FWI values calculated based on the Canadian Fire Weather Index system in ERA5 (Vitolo et al. 2020; Wagner et al. 1987). The FWI used in this study takes ERA5's temperature, relative humidity, wind speed and 24-h precipitation to provide numeric ratings for the potential of wildland fire (Van Wagner et al. 1987). The FWI comes from an integration of an Initial Spread Index, which uses temperature, relative humidity, precipitation, and wind data, and a Buildup Index which uses temperature, relative humidity, and precipitation. Details on the calculation of each index can be found in Van Wagner et al. (1987). In addition to the FWI, we provide composites of 2-m temperature (T2m), 2-m dewpoint temperature (D2m) and 10-m winds (both zonal and

meridional components from ERA5). As the FWI is calculated using local noon values, T2m, D2m and 10-m winds at 18:00 UTC are used to represent as close to local noon as possible for North America. These values are composited as anomalies from their respective daily climatology (1979–2020). Finally, daily precipitation anomalies are evaluated from the Climate Prediction Center's Global Unified Gauge-Based Analysis data with 0.5° resolution over land.

## 3 Typhoon classification

We include tropical cyclones from 1979 through 2020 which reached a typhoon classification (sustained winds greater than 32.8 m/s) and an extratropical cyclone classification by the JMA. This ensures that each typhoon in our analysis had interactions with the extratropical flow. The start date is chosen as 1979 because the Best Track Data started classifying typhoons which became extratropical low-pressure systems in 1977, making categorical grouping of typhoons more efficient and objective, and this period overlaps with satellite era reanalysis data as well. The reference point used to view the time-lagged impact of an ETC is defined as the point in which an ETC passes 30° N. As it has been shown that an ETC may start to impact the jet region before the extratropical transition (Stuivenvolt-Allen et al. 2021), this latitude threshold produced more clearly defined wave trains in the composite maps than selecting the point of ETC recurvature (not shown). The latitude requirement also reduces the potential for the composite maps to contain lower-latitude/tropical forcing mechanisms similar to the Pacific-North America teleconnection (Wallace et al. 1993). A latitude requirement for the reference time-step (T0) also results in better defined atmospheric wave trains.

### 3.1 Composite analysis

To delineate the general impact of typhoons on fire weather and North American circulation we create composite maps of FWI and z200 anomalies. All anomalies are defined as the deviation of the daily value from their respective daily climatology (1979–2020). First, we composited two-day means of z200 and FWI anomalies for 7 days after T0 to visualize the evolution of both variables during an ETC lifetime. We elected to use two-day means of these variables as the differences from day-to-day following T0 are quite small (not shown) and we aimed to emphasize enhanced FWI conditions that persist for longer than one day. An evolution of these two-day means is provided in the supplement (Figure S1 and S2). As the composites which lag T0 by 3–4 days (hereafter referred to as T + 4) show that the circulation anomalies have translated across the North Pacific and over North America, we will use this time-step for the subsequent analysis. Additionally, as the atmospheric upper-level flow is most amplified about two-to-four days after typhoon recurvature in the north Pacific (Archambault et al. 2013), this lag time most effectively captures the amplified pressure field and potential for enhanced fire weather. ETCs are subsequently grouped by July through August (JA) and September through October (SO) so that the seasonal characteristics of the jet stream and ETCs are separated. Finally, to reduce smearing effects in the composite maps due to differences in the ETC location, each ETC and its associated z200 and FWI anomalies are grouped by quartiles (Q1–Q4) of T0 longitude (Figure S1 and S2). Subsequently, the composite fields are averaged into four groups based off the longitudinal location of the ETC at T0. This allows for the comparison of equitable sample sizes and results in groups of ETCs that occurred within similar locations.

To evaluate the efficacy of this longitudinal grouping and of the selection of the T0 start time, supplemental Figure S1 displays the composite z200 anomalies for three time-steps out to six days following T0. To the northeast of each T0 point (the longitudinal quartiles are shown by gray rectangles), enhanced ridging is occurring due to the diabatic outflow of each ETC. Adjacent to the localized ridge produced by the ETC is extratropical cyclogenesis and the formulation of a Rossby wave train across the North Pacific. It is notable that the z200 anomalies are more pronounced for SO, which is likely a product of the stronger jet for this season (Finocchio and Doyle 2019). In summary, the longitudinal and seasonal grouping of typhoons effectively produces the circulation features expected for the initial interaction of a ETC with the jet region. Additionally, we can see the wave packet associated with ETC is impacted by the longitudinal position of recurvature.

As a final validation measure, we created composites of FWI and z200 for a control group with no ETCs. First, we found 10-day periods where no tropical storms, typhoons or ETCs were logged by the JMA Best Track data. We then created composites of days without these disturbances by randomly sampling 100 cases of z200 and FWI anomalies during these days.

## 4 Results

### 4.1 Impact of typhoon position and season on downstream fire weather

The spatial density of ETCs is shown in Fig. 1, with the track density of the typhoon trajectories for July through October. This shows that the heaviest density of ETCs occurs just south of Japan, but ETCs span a longitudinal range from 120° E to about 170° E. Also plotted in Fig. 1 is the climatological FWI distribution in North America from July

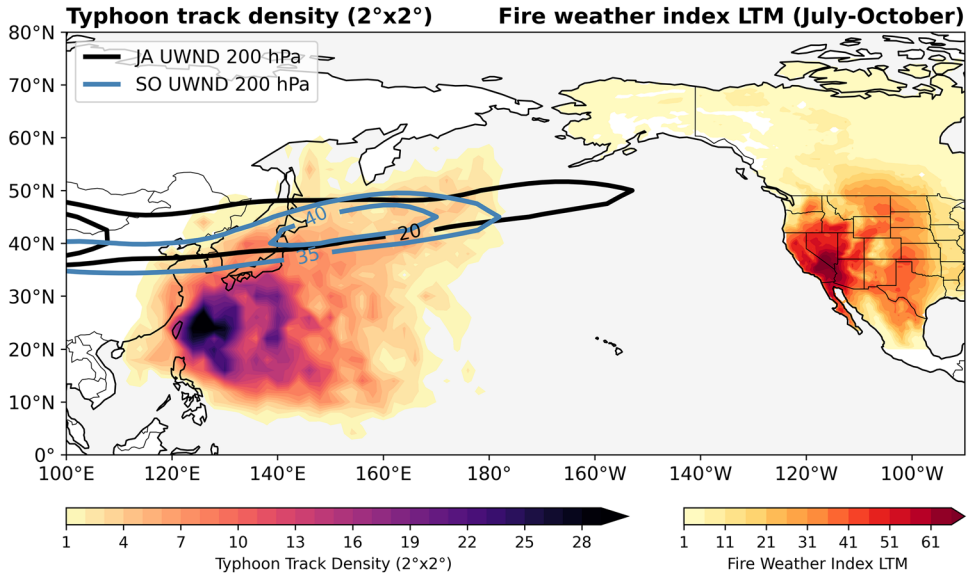


**Fig. 1** Typhoon track density (shading in the western Pacific) of ETCs along with the long-term mean jet stream (1981–2010) for JA and SO (contours). The shading over North America represents the long-term mean FWI from 1981 to 2010

through October, showing that the Southwest United States has a consistently high FWI through these months. The FWI is a unitless and open-ended index, so the climatology serves as a reference point for the subsequent analysis. The positions of the long-term mean jet stream cores in JA and SO are shown in the contours. While the position of the jet stream does not experience a major shift from JA to SO, the jet intensity is notably higher for SO. As a stronger jet results in a higher-amplitude Rossby wave response (Finocchio and Doyle 2019), all future analysis will be split into the two seasons to better isolate the signal associated with an ETC.

Figure 2 shows composites of z200 and FWI for our control days without ETCs (Fig. 2a, b) compared with all of the ETC days (Fig. 2c, d). Both the JA and SO control composites do contain isolated areas of significant FWI anomalies. However, when comparing these control composites to the ETC composites in Fig. 2c, d, the area of affected FWI anomalies is much greater in the ETC composites. Importantly, large areas of reduced FWI are present in much of North America for the ETC composites. These are collocated with either negative or near normal z200 anomalies and highlight that ETCs can reduce or intensify fire weather risk.

While Fig. 2 shows that ETCs in aggregate appear to modulate North American fire weather, the rest of our analysis will evaluate the role of different ETC characteristics in impacting downstream FWI responses. First, typhoons are grouped into four longitudinal bins based on their quartile ranges. The first three longitudinal bins (shown as gray rectangles in Fig. 3) each contain 25% of the ETCs used in this analysis for the respective season. The fourth longitudinal bin, which contains the largest range, is limited to be 10° greater than the 3rd quartile. As the total range of the fourth longitudinal bin was approximately 30° in longitude, we aimed to reduce the spatial heterogeneity of ETCs in this group to be more comparable with the first three quartile bins. The quartiles are computed for ETCs in JA, and again for SO due to the seasonal shifts of recurving typhoons. Generally, the position of recurvature moves southeast from July through September (Archambault et al. 2013).

Additionally, to evaluate the seasonal differences in the downstream FWI response to ETCs, Fig. 3 shows the composite anomalies for T + 4 for July through August ETCs for each longitudinal position (Fig. 3a–d), alongside September to October ETCs (Fig. 3e–h) for z200 and FWI. For JA, the z200 composite response depicts an enhanced ridge over the Gulf of Alaska, with a negative pressure anomaly over the west coast of the US. Even with changes in the longitudinal position of T0, z200 anomalies three-to-four days after T0 are only marginally shifted over North America (Fig. 3a–d). The most notable and widespread increase in FWI is observed in the center of the North American continent, with amplified FWI shown near the Great Plains (Fig. 3a–d), the eastern slopes of the Rockies (Fig. 3a–d), and North Western Canada (Fig. 3d). These are overlaid by positive z200 anomalies. Negative FWI anomalies are observed along the west coast of North America (Fig. 3a–c) and around Texas and the Gulf states (Fig. 3b, d). These are overlaid by negative z200 anomalies.

The downstream response in SO shows similar features, with positive FWI collocated with high-pressure anomalies and negative FWI generally associated with low-pressure anomalies. The ridge location adjacent to North America also appears more sensitive to the longitude of recurvature for SO, with the maximum downstream ridge shifting east along with the longitude of T0 (most notable in Fig. 3e–g). Areas of enhanced FWI are seen adjacent to low-pressure

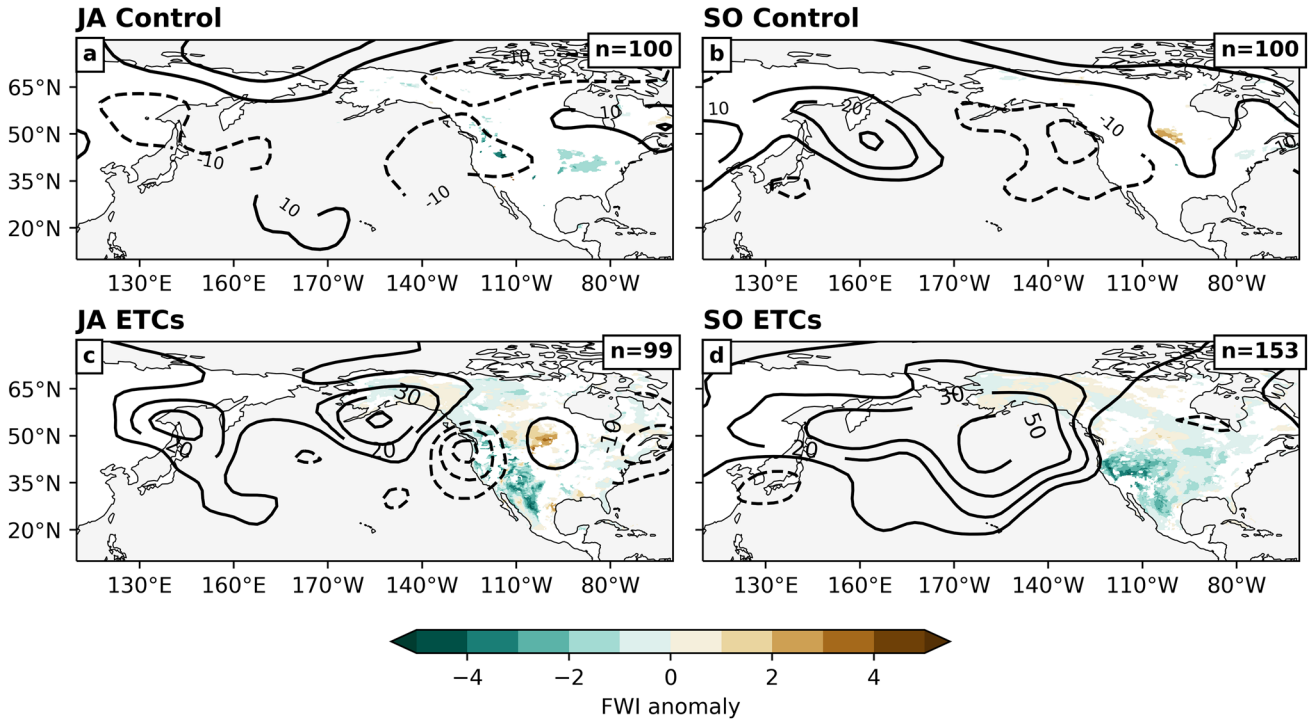


**Fig. 2** Composite z200 and associated FWI for the control group and for ETCs in JA and SO at T + 4 (an average of the 3rd and 4th day following T0). Composites for the control, no-ETC days are shown in 2a and 2b, while composites for ETC days are shown in 2c and 2d. Only FWI values which are determined to be statistically different (using a two-sided Student's t-test) from the climatological values at each grid point are plotted ($p < 0.05$)

anomalies as well (Fig. 3f, h), suggesting that the enhanced fire weather conditions associated with ETCs may be linked to wind events rather than rapid temperature or humidity changes alone. Generally, it appears that ETCs which recurve farther west (Q1 and Q2) tend to result in FWI anomalies in the Northern Intermountain West (Fig. 3a, b) and Great Plains (Fig. 3b, f) and along the eastern side of the southern Rocky Mountains (Fig. 3a, b, e, f). Modulation of FWI activity in the Pacific Northwest on the other hand is more common with ETCs that recurve farther east (Q4 of JA and Q3 and 4 of SO).

The composite analysis highlights that fire weather responses in North America are localized and scattered. However, the composites do not provide much insight into the spread or variability within each composite group. Therefore, we show the composite members in Fig. 4, which are included in Fig. 3b. ETCs which recurve in the same longitudinal quartile can produce different downstream responses, noted by the large spread in z200 and FWI response in Fig. 4. As a result, FWI anomalies are not remarkably consistent based on the grouping of ETCs (Fig. 3b). Circulation features change substantially from case-to-case as well, but elements of the composite means can be noticed in these individual cases, namely a negative pressure anomaly which is commonly featured just off or over the western coast of North America. Again, amplified FWI anomalies are generally found under anomalous ridging and negative FWI anomalies are under and adjacent to troughs. One caveat is that amplified FWI is occasionally seen on the southwest axis of a trough, likely because of anomalous winds around the frontal boundary.

Figure 5 shows 25 random members of the composite for Q4 in SO. While the composite average shows almost no significant FWI anomalies in the southwestern United States, we can see that individual members are associated with FWI anomalies in this region (see examples during October 13, 1984, and September 27, 1994). However, there is little agreement on the precise region of positive FWI changes for this grouping of ETCs. Like the cases in Fig. 4, there are often amplified FWI anomalies under high-pressure regions with some localized enhancement at certain frontal boundaries (see the cases for October 31, 1994, and October 25, 2013). This highlights the difficulty of synthesizing general impacts of ETCs on fire weather, as ETCs which occur in similar seasons and at similar locations can have differing downstream impacts.

Consistent FWI anomaly patterns appear in the composite analysis for Fig. 3, but the many distinct patterns present in the FWI anomalies in Figs. 4 and 5 suggest that ETCs may also result in altered variance in FWI anomalies

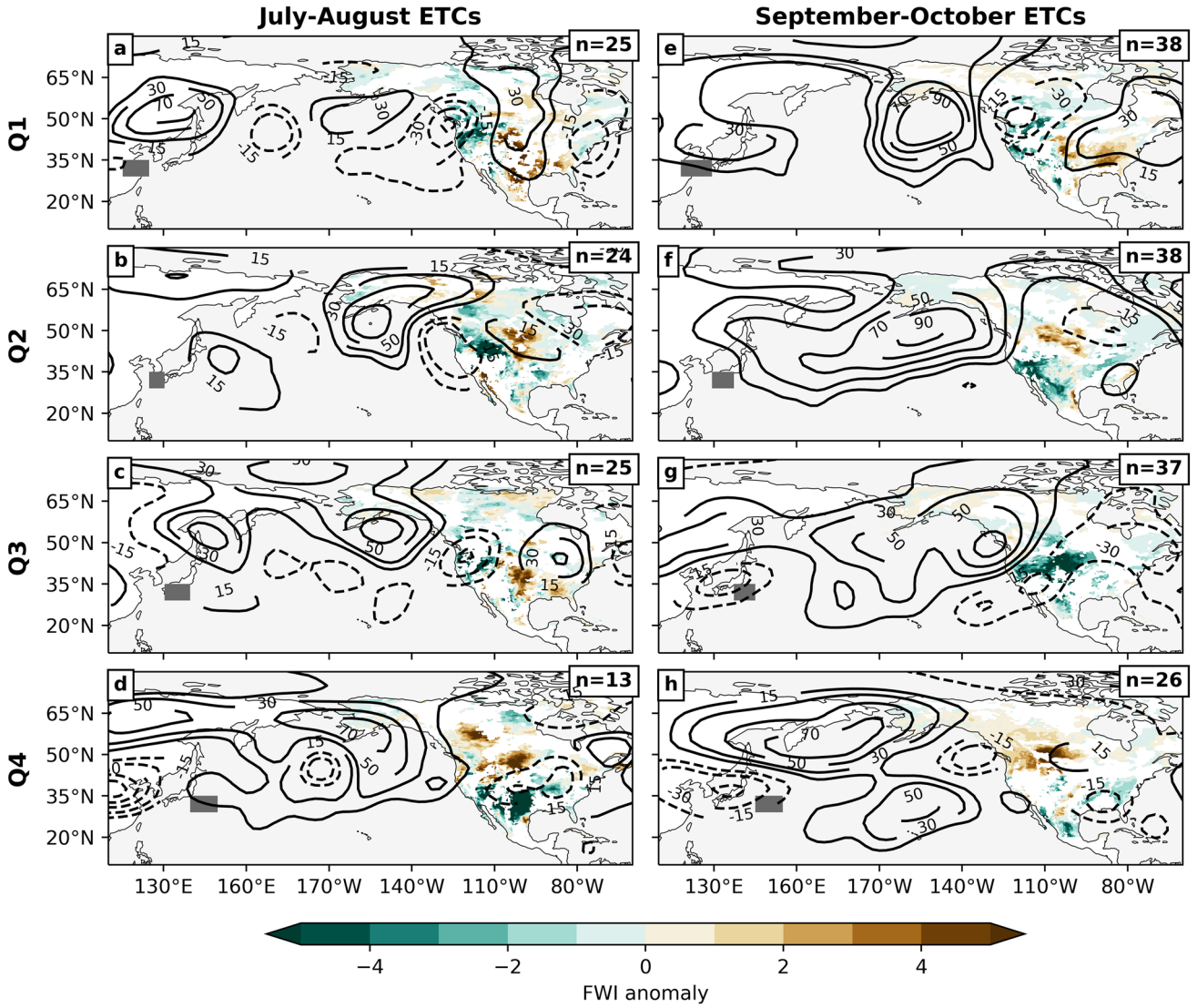


**Fig. 3** Composite z200 and FWI associated with ETCs for JA (**a–d**) and SO (**e–h**) for 3–4 (T+4) days after T0. The gray boxes indicate the quartile ranges for T0 longitude for the respective season. A Student's t-test is used to determine which areas have mean FWI values that are significantly different than climatological values for the same days. Only values which surpass the 95% confidence interval are shown for FWI

rather than consistent FWI anomalies of the same sign. To test this, we compare the difference between the FWI anomaly variance from these composites to the FWI anomaly variance from the control cases (Figure S3). The composite technique does not appear to be washing out too much of the FWI variability as the largest increases in FWI anomaly variance (Figure S3) overlap with regions that have the largest composite FWI anomaly values (Fig. 3). In conclusion, while case-to-case FWI anomalies differ between ETCs of similar longitudinal quartiles, the composite methods adequately highlight regions were mean FWI anomalies are amplified or diminished with respect to specific longitudinal positions of ETCs.

## 4.2 Impact of ETC strength

Archambault et al. (2013) also showed that stronger ETCs, by measure of their central MSLP and the radius of the 30 kt winds, produce a more amplified flow response. Generally consistent with this finding, we show the intensity of an ETC has an impact on the interaction with the jet region and the amplitude of the local ridge amplification at T0 (Figure S4). Figure S4 shows that ETCs which have lower minimum central MSLP (Figure S4a–d) tend to produce a more amplified local ridge than ETCs with higher central MSLPs (Figure S4e–h). However, these differences are only prevalent for the z200 anomalies in the western Pacific around T0, while

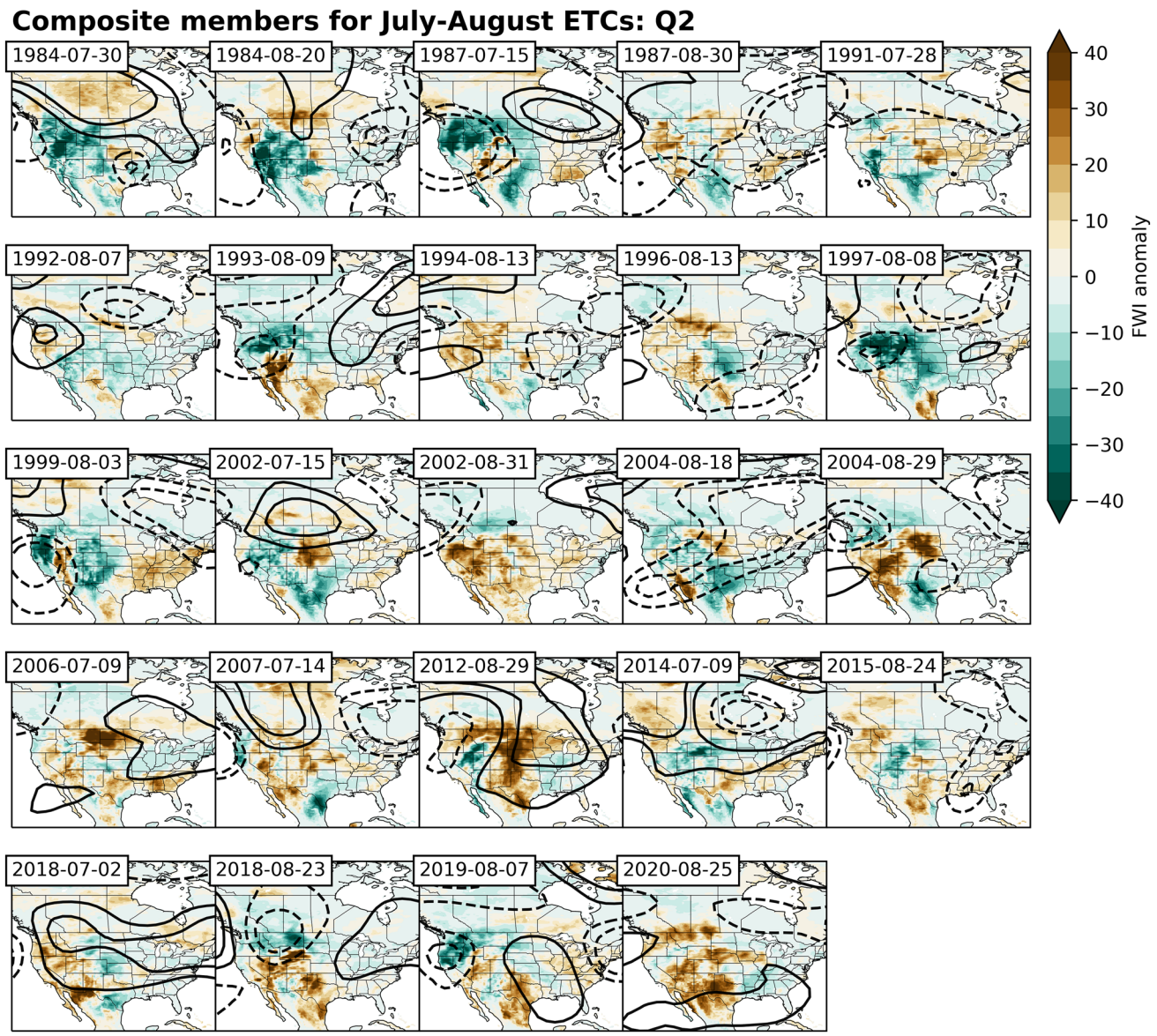


**Fig. 4** FWI and z200 anomalies associated with the twenty-four composite members from Q2 of ETC longitude for JA. The solid and dashed contour lines respectively indicate a 70 m and 140 m anomaly in z200 from the daily long-term mean. The dates are organized from left-to-right then top-to-bottom

the eastern north Pacific at T + 4 (150–110° W) shows a less coherent response to ETC based on MSLP (Fig. 6). It is possible that this composite analysis better depicts the western North Pacific z200 response to an ETC, but the z200 anomalies in the eastern Pacific which are further away from the initial perturbation may become more divergent. Subsequently, there is not a clear relationship between ETC MSLP at T0 and the downstream fire weather or downstream z200. While regions of anomalous FWI are still captured in Fig. 6 (most notable in Fig. 6c), comparing the group of strong and weak ETCs shows that intensity does not consistently impact the FWI response. The composites for JA produce analogous results and are omitted for brevity. Finally, composites of the 30-kt wind radius also result in no significant modulation of FWI anomalies.

### 4.3 Impacts of the jet stream interaction

While the position and timing of ETCs within the seasonal cycle has been shown to have an effect on the magnitude of north Pacific flow amplification (Archambault et al. 2013; Evans et al. 2017), our composite analysis has highlighted that these seasonal and location characteristics do not consistently alter fire weather at any one location in North America. It is possible that our grouping of ETCs does not account for critical factors which influence the exact position

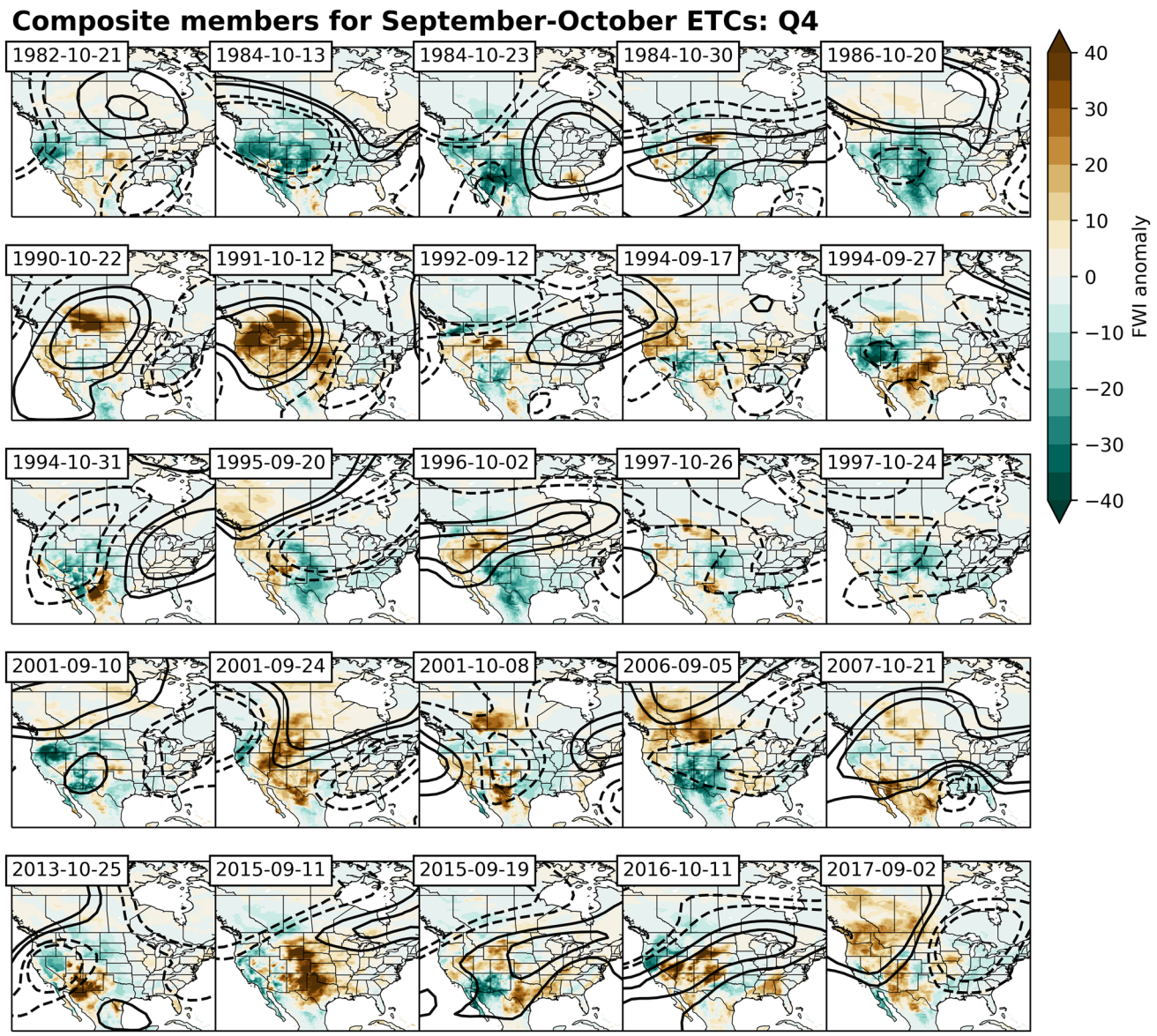


**Fig. 5** Same as Fig. 4, but for 25 randomly selected cases from Q4 of SO

of synoptic features. Literature about ETC impacts on north Pacific flow regimes has also shown that the background conditions in which an ETC occurs are fundamental for the potential of amplified flow. In particular, an ETC is more likely to result in downstream impacts if the interaction with the mid latitude flow is constructive—meaning the ETC can amplify already existing wave trains or synoptic pressure patterns (Evans et al. 2017; Jones et al. 2003). Additionally, the impact of an ETC is greater when the interaction with the jet stream is stronger (Archambault et al. 2013, 2015). The potential vorticity (PV) framework is commonly utilized to analyze the interaction between an ETC and the jet, as the diabatic heating from an ETC results in low PV advection into the jet region which is considered the initial perturbation that eventually results in a Rossby wave train across the Pacific. The strength of the ETC and jet interaction can therefore be characterized using the PV framework, where strong interactions result in more widespread and negative values of PV advection into the jet region (approximately 200 hPa in summer) (Bosart et al. 2017; Bosart and Lackmann 1995; Molinari et al. 1997).

Figure 7 shows the response of grouping cases of ETCs by the strength of their interaction with the jet stream upon extratropical transition for JA and SO. The 200 hPa PV advection is computed for the time step in which an ETC was first categorized as an extratropical low-pressure system. To quantify the interaction, the negative PV advection was summed within a domain surrounding the location of

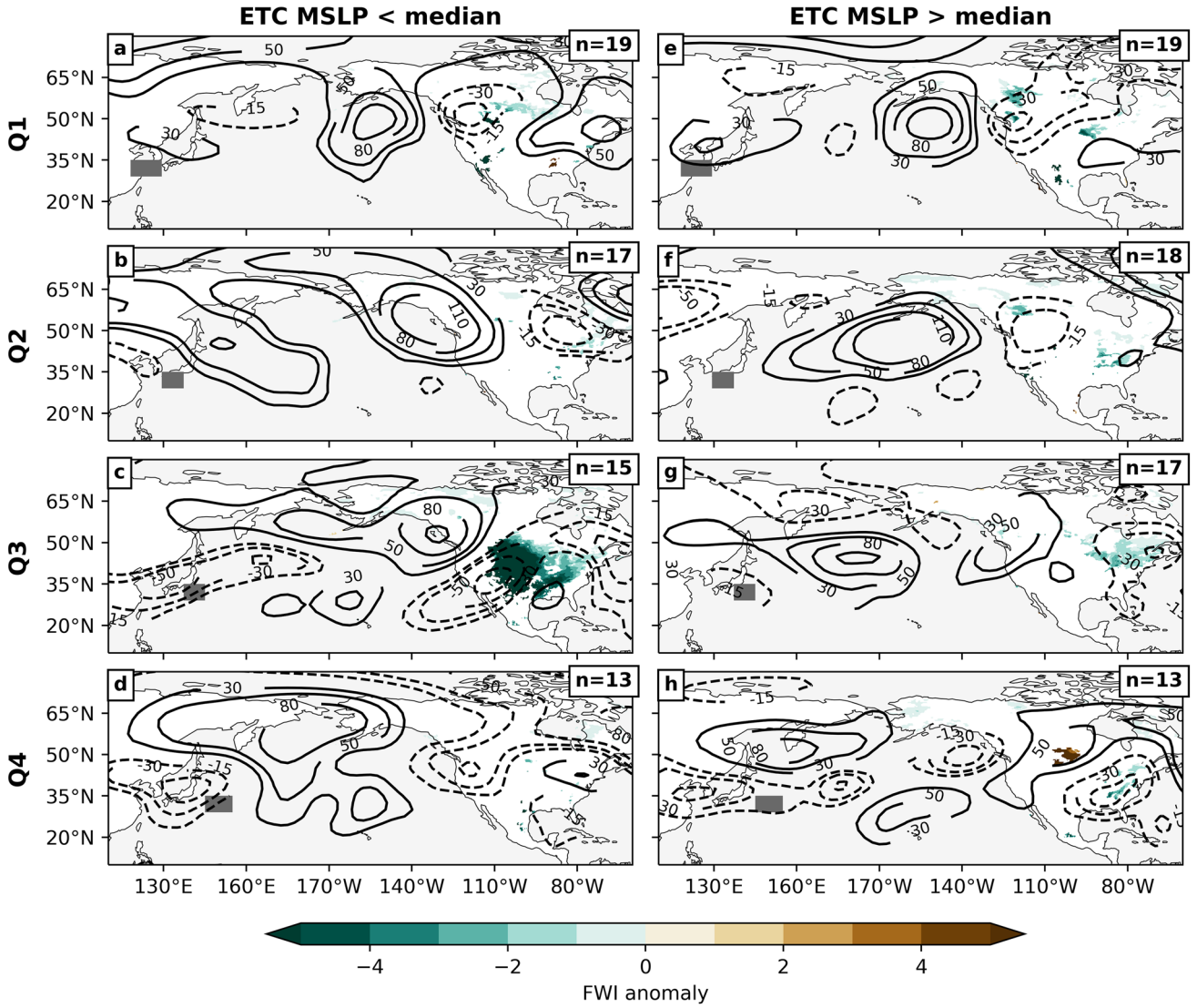


**Fig. 6** Composite z200 and FWI at T+4 associated with ETCs which occurred in SO. **a–d** Composites anomalies of z200 and FWI for ETCs with a central MSLP below the median for each longitudinal quartile. **e–h** The composite response for ETCs with a central MSLP greater than the median for each longitudinal quartile. The gray boxes indicate the quartile ranges for T0 longitude for the respective season. Only FWI values which surpass the 95% confidence interval are shown

the ETC central pressure anomaly (20° W–20° E and 5° S–20° N of the ETC). The domain was chosen by plotting cases of negative PV advection and selecting a boundary that captured the entire impact of the ETC. After determining the median negative PV advection from all cases, the ETCs are separated into strong (more negative PV advection) and weak (less negative PV advection) groups. As this analysis is centered by the minimum central pressure, Fig. 7 is not broken into longitudinal quartiles. In Fig. 7, the composite PV advection for the ETCs which had strong interactions with the jet stream depicts broader and more negative PV advection. The maximum point of interaction is to the northwest of the center of each ETC. The SO interactions are notably more intense which may be a product of enhanced jet stream speeds for these months (Finocchio and Doyle 2019).

The z200 anomalies for both the strong and weak jet interactions are not clearly distinct for JA, and neither is the associated fire weather (Fig. 8). FWI anomalies are mostly insensitive to the strength of an ETC and jet stream interaction, though larger areas of reduced FWI are seen during the weaker interactions in JA (Fig. 8e–g). As the strong PV interaction composites show only sparse significant changes in FWI anomalies, it appears ETC characteristics (aside from the location of the storm) are not associated with markedly consistent changes to the FWI response in North America. Like the findings from Fig. 3, the JA z200 anomalies do not drastically shift in response to changes in the longitudinal

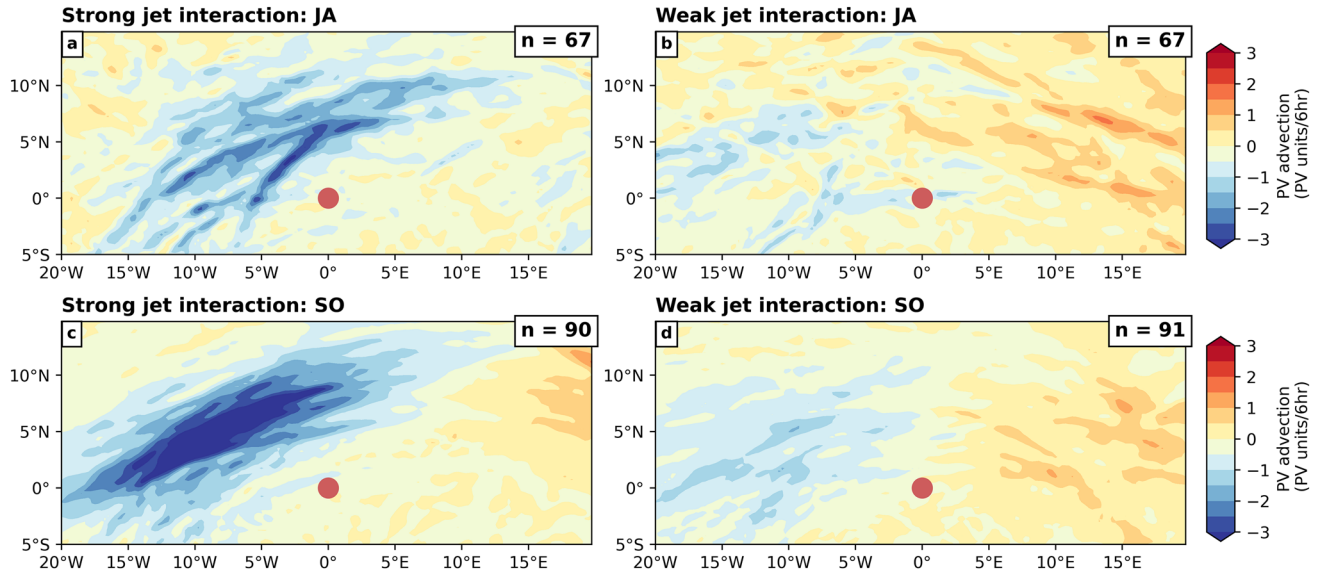


**Fig. 7** Average PV advection for all ETCs analyzed in this study with a strong jet interaction (**a**, **c**, negative PV advection less than the median) and a weak jet interaction (**b**, **d**, negative PV advection greater than the median) during JA (**a, b**) and SO (**c, d**). The contour plot shows the PV advection relative to the center of the ETC, represented by the red dot. PV is represented by PV units, which is defined as $m^2\ s^{-1}\ K\ kg^{-1}$ multiplied by 1.0e6. Note that the contour range is increased for the SO composites

quartiles of ETCs. Almost all the composites feature a ridge in the Gulf of Alaska and a trough over the Pacific Northwest (Fig. 8a–g). The composites for SO—also lacking a notable difference in the FWI anomalies between strong and weak ETC-jet interactions—are included in the supporting information as Figure S5. The eastward movement of the downstream ridge along with the longitude of the ETC at 30° N is much more prominent in the SO cases with strong PV interactions when compared to weak PV interactions (Figure S5).

### 4.4 Meteorological conditions associated with ETC driven fire weather

Figure 9 investigates the meteorological conditions associated with the amplified flow regime from an ETC for JA. The four meteorological variables that are used in calculating the FWI, T2m, D2m, 10-m wind, and precipitation, are composited for each longitudinal quartile. These variables are critical for fire weather conditions as they can quickly alter vapor pressure deficits, fuel moisture, and fire spread potential. To evaluate which variables most closely align with the significant FWI anomalies, stippling is overlaid on the composite maps to denote where FWI anomalies were significantly positive (dots) and negative (lines) from the composite analysis in Fig. 3. In the case of 10-m winds which are displayed as vectors in Fig. 9c, red shading indicates significantly positive FWI anomalies ($p < 0.05$) and blue shading indicates negative. While there are overlaps in the largest anomalies of each field and the significant FWI anomalies, there are also locations where the direction of the anomaly does not agree (i.e. lower dewpoint temperatures in an area with negative fire weather anomalies in the Pacific North West of Q1, Fig. 9b). There is a clear association between T2m anomalies and the location of positive and negative FWI anomalies (Fig. 9a–d), but anomalies of D2m, wind, and precipitation are not holistically consistent with the location of positive and negative FWI anomalies. Figure 9 therefore highlights some of the challenges in evaluating the fire weather response to amplified flow regimes induced by ETCs, that is, there are a myriad of conditions that may culminate in locally enhanced fire weather and no one primary variable can describe observed fire weather potential. From a composite perspective however, the most important associated change in fire weather associated with an ETC appears to be driven by T2m anomalies associated with altered circulation over North America. Composite averages of these meteorological variables are included for SO in Figure S6 and for the control days with no ETCs in Figure S7.

## 5 Discussion and conclusions

Western North Pacific ETCs have been extensively documented for their impact on amplified flow regimes and extreme weather events in North America, most notably cold-air outbreaks and precipitation extremes (Bosart et al. 2017; Grams et al. 2013; Jones et al. 2003). We have shown that these impacts include enhanced or suppressed fire weather conditions for much of North America as well,

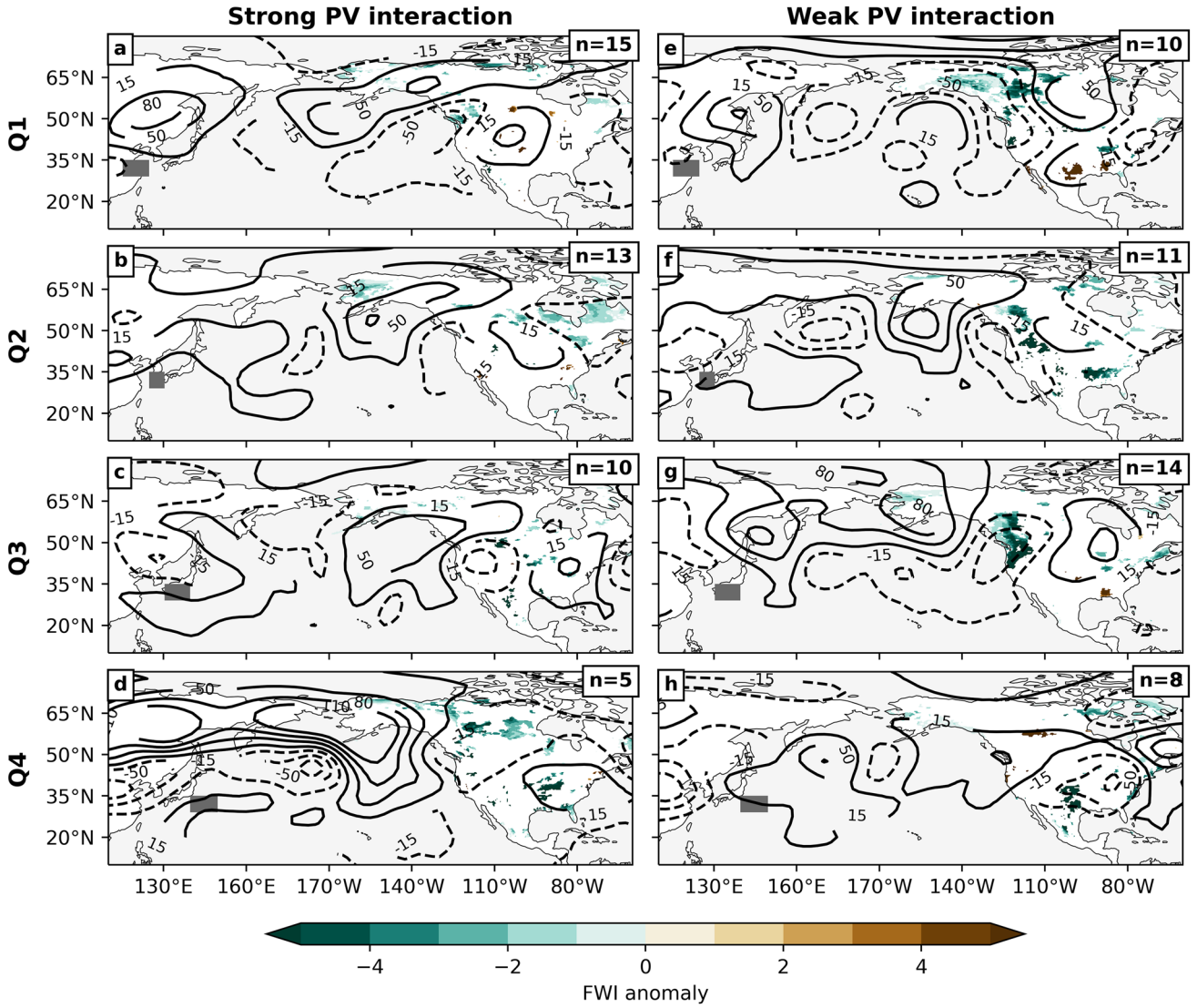


**Fig. 8** Composite z200 and FWI anomalies at T+4 associated with ETCs which occurred in JA. **a–d** Composites anomalies of z200 and FWI anomalies for ETCs characterized by a strong jet interaction. **e–h** The composite response for ETCs with a weak jet interaction. The gray boxes indicate the quartile ranges for T0 longitude for the respective season. Only values which surpass the 95% confidence interval are shown for FWI

made likely by the simultaneous occurrence of peak ETC and fire seasons. However, composite analysis of ETCs and their associated fire weather conditions highlights that the downstream response to ETCs is chaotic and varied. ETCs which occur in the same region and season can produce different downstream responses due to minor shifts in the north Pacific Wave train. Fire weather in particular is often enhanced or suppressed on small scales and over small geographic features, likely due to the heterogenous distribution of forests and fuels and topographical impacts on surface winds (Krawchuk et al. 2016). As a result, small shifts in the amplified flow pattern can cause large shifts in the location and intensity of anomalous fire weather conditions.

From a composite perspective, we conclude that the impact of an ETC on fire weather is most prominently caused by the associated temperature anomalies from altered circulation regimes as enhanced FWI values are almost exclusively associated with high-pressure anomalies and the spatial pattern of significant FWI most closely matches composites of T2m. Simply, the position of ridging in the north Pacific wave train is generally the catalyst for enhanced fire weather, as anomalously hot conditions can result in more fire-prone fuel loads and vapor pressure deficits (Keen et al. 2020; Seager et al. 2015). The composite analysis also highlights that the Pacific Northwest, upper Intermountain West, and the eastern slopes of the Rocky Mountains have the most consistent fire

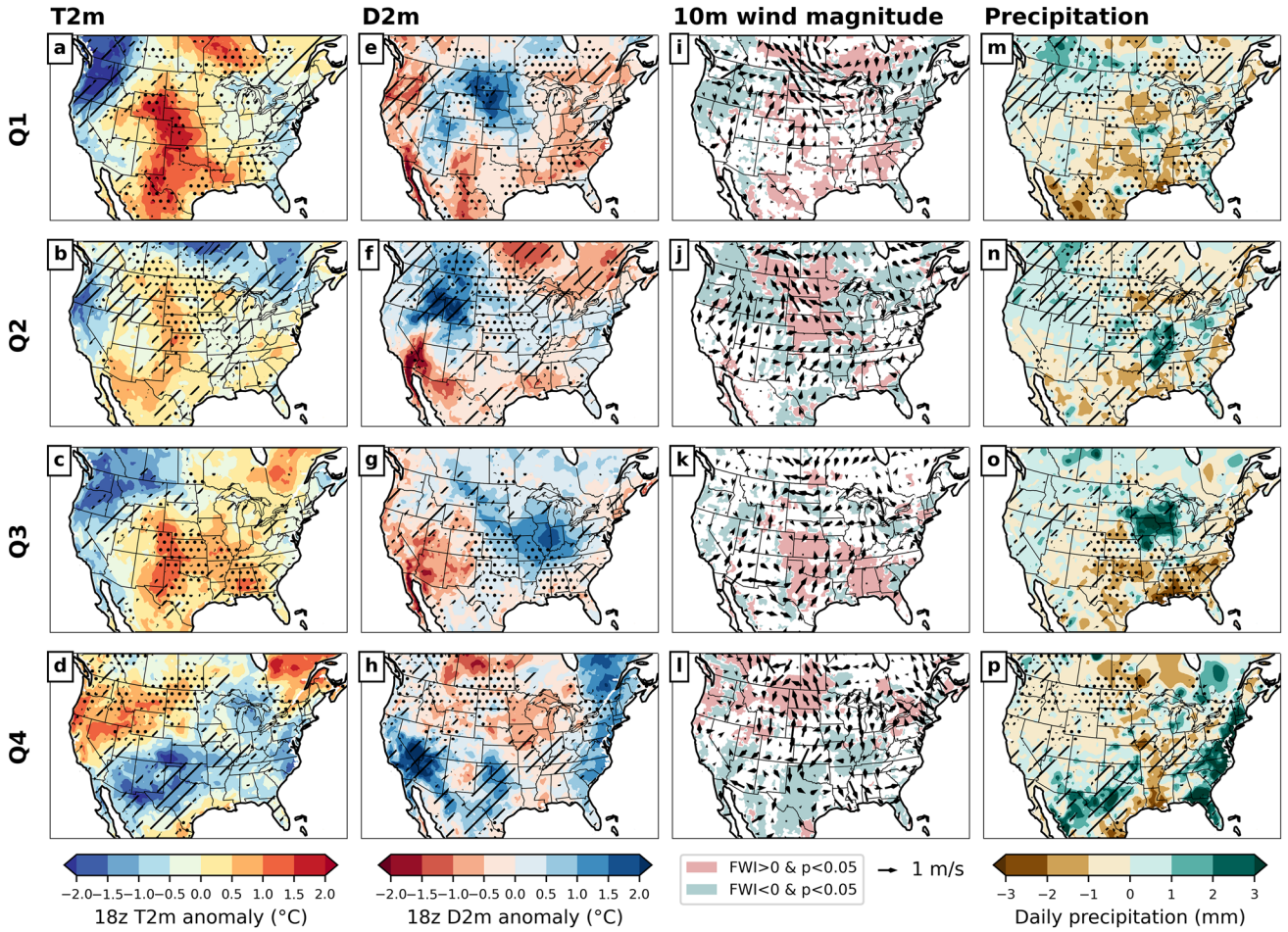


**Fig. 9** Composite T2m (**a–d**), D2m (**e–h**), 10-m winds (**g–j**), and precipitation anomalies (**p–m**) at T + 4 for Q1–Q4 of JA. For the T2m, D2m and Precipitation columns, stippling indicates the regions of significantly positive FWI anomalies while the diagonal lines indicate the regions of significantly negative FWI anomalies. For the wind magnitude column, the red (light blue) shading marks areas of corresponding FWI anomalies which are significantly positive (negative)

weather response to ETCs (Fig. 3). The climatology of FWI in Fig. 1 shows that these regions have a lower fire weather risk compared to the Southwest United States, but the impact of an ETC can result in anomalous spikes or decreases in fire weather. For JA, the location of downstream ridging is quite insensitive to the longitude at which an ETC enters the mid-latitudes, with most z200 anomaly composites presenting a ridge over the Gulf of Alaska and a trough along the west coast of North America. In SO however, the synoptic circulation features change more consistently with the longitude of an ETC—the wave packets migrate east along with the longitude of the ETCs emergence into the midlatitudes—possibly due to increased jet speeds. While the exact mechanism for this seasonal difference requires further exploration, the different jet stream intensities between JA and SO have been shown to affect the downstream response to ETCs at varying longitudes (Finocchio and Doyle 2019).

With the well-documented increase in wildfire severity and intensity, largely a result of climate change, forest management practices, and shifts in ignition to more anthropogenic causes (Abatzoglou and Williams 2016; Balch et al. 2017; Collins et al. 2019; Harvey 2016; Holden et al. 2018; Jain et al. 2017; Westerling 2016; Yoon et al. 2015), the relationship between ETCs and actual fire events could be changing too. Even without the impact of climate change, upstream perturbations might exacerbate already enhanced fire conditions that are caused by internal climate variability (Gedalof 2011; Schoennagel et al. 2007; Westerling and Swetnam 2003). Additionally, ETCs have been shown to decrease forecast skill for about a week after recurvature, a direct influence on tools that are crucial for fighting and containing existing fires (Aiyyer 2015; Grams et al. 2015; Jones et al. 2003).

The findings of this study are limited using a mostly Eulerian analysis framework. Without using Lagrangian

techniques, it is difficult to document the impacts of background flow conditions on the downstream weather response (Archambault et al. 2015; Bosart et al. 2017). One unexplored factor is the phase locking of an ETC with nearby troughs, which has a role in determining whether the ETC perturbation is constructive to existing Rossby waves (Riboldi et al. 2019). Our analysis shows that FWI responses are generally unpredictable based off ETC characteristics alone, but more clear relationships between FWI variability and ETCs may be established by evaluating the response of FWI to ETCs through the background circulation regimes. While our analysis does not adequately account for all the complexity and potential forcing mechanisms involved in the relationship between ETCs and downstream weather, we provide a baseline for further research and exploration. Future work will aim to document the background flow conditions and how they influence the realization of fire weather or weather extremes in North America. Additionally, the impacts of seasonal and inter-annual climate variability on the ETC-jet stream interaction are currently unexplored and may further impact the likelihood of downstream weather extremes.

**Supplementary Information** The online version contains supplementary material available at https://doi.org/10.1007/s00382-022-06561-1.

**Author contributions** JSA performed all data analysis in this paper. Methodology was determined by JSA and SYSW. Interpretation of analysis was aided by all authors. Data acquisition was undertaken by JSA. The first draft of the manuscript was written by JSA and all authors provided comments, edits and additional writing. The final manuscript has been read and approved by both authors.

**Funding** We acknowledge research funding from the U.S. Department of Energy/Office of Science under Award Number DE-SC0016605 and the SERDP project RC20-3056. JSA was supported by the National Science Foundation under Grant No. 1633756. SYSW was also supported by the U.S. Department of Interior, Bureau of Reclamation with Grant No. R19AP00149.

**Data availability** All data used in this study can be acquired free of charge to any member of the public or by request to the corresponding author. The code used in this study can be requested from the corresponding author, at jacob.stuivenvolt-allen@yale.edu.

## Declarations

**Conflict of interest** The authors have no conflicts of interest to declare that are relevant to the content of this article.

**Ethical approval** The authors declare no competing interests and consent to participate or consent to publish declarations are not applicable given the scope of this research.

## References

Abatzoglou JT, Williams AP (2016) Impact of anthropogenic climate change on wildfire across western US forests. Proc Natl Acad Sci 113(42):11770–11775. https://doi.org/10.1073/pnas.1607171113

Agustí-Panareda A, Gray SL, Craig GC, Thorncroft C (2005) The extratropical transition of tropical cyclone Lili (1996) and its crucial contribution to a moderate extratropical development. Mon Weather Rev 133(6):1562–1573. https://doi.org/10.1175/MWR2935.1

Aiyyer A (2015) Recurving western North Pacific tropical cyclones and midlatitude predictability. Geophys Res Lett 42(18):7799–7807. https://doi.org/10.1002/2015GL065082

Archambault HM, Bosart LF, Keyser D, Cordeira JM (2013) A climatological analysis of the extratropical flow response to recurving western north pacific tropical cyclones. Mon Weather Rev 141(7):2325–2346. https://doi.org/10.1175/MWR-D-12-00257.1

Archambault HM, Keyser D, Bosart LF, Davis CA, Cordeira JM (2015) A composite perspective of the extratropical flow response to recurving western north pacific tropical cyclones. Mon Weather Rev 143(4):1122–1141. https://doi.org/10.1175/MWR-D-14-00270.1

Balch JK, Bradley BA, Abatzoglou JT, Nagy RC, Fusco EJ, Mahood AL (2017) Human-started wildfires expand the fire niche across the United States. Proc Natl Acad Sci 114(11):2946–2951

Barcikowska M, Feser F, von Storch H (2012) Usability of best track data in climate statistics in the western North Pacific. Mon Weather Rev 140(9):2818–2830. https://doi.org/10.1175/MWR-D-11-00175.1

Bosart LF, Lackmann GM (1995) Postlandfall tropical cyclone reintensification in a weakly baroclinic environment: a case study of hurricane David (September 1979). Mon Weather Rev 123(11):3268–3291. https://doi.org/10.1175/1520-0493(1995)123%3c3268:PTCRIA%3e2.0.CO;2

Bosart LF, Moore BJ, Cordeira JM, Archambault HM (2017) Interactions of North Pacific tropical, midlatitude, and polar disturbances resulting in linked extreme weather events over North America in October 2007. Mon Weather Rev 145(4):1245–1273. https://doi.org/10.1175/MWR-D-16-0230.1

Collins L, Bennett AF, Leonard SWJ, Penman TD (2019) Wildfire refugia in forests: severe fire weather and drought mute the influence of topography and fuel age. Glob Change Biol 25(11):3829–3843. https://doi.org/10.1111/gcb.14735

Evans C, Wood KM, Aberson SD, Archambault HM, Milrad SM, Bosart LF, Corbosiero KL, Davis CA, Dias Pinto JR, Doyle J, Fogarty C, Galarneau TJ, Grams CM, Griffin KS, Gyakum J, Hart RE, Kitabatake N, Lentink HS, McTaggart-Cowan R, Zhang F (2017) The extratropical transition of tropical cyclones. Part I: cyclone evolution and direct impacts. Mon Weather Rev 145(11):4317–4344. https://doi.org/10.1175/MWR-D-17-0027.1

Finocchio PM, Doyle JD (2019) How the speed and latitude of the jet stream affect the downstream response to recurving tropical cyclones. Mon Weather Rev 147(9):3261–3281. https://doi.org/10.1175/MWR-D-19-0049.1

Gedalof Z (2011) Climate and spatial patterns of wildfire in North America. In: McKenzie D, Miller C, Falk DA (eds) The landscape ecology of fire. Springer, Amsterdam, pp 89–115. https://doi.org/10.1007/978-94-007-0301-8_4

Grams CM, Jones SC, Davis CA (2013) The impact of typhoon Jangmi (2008) on the midlatitude flow. Part II: downstream evolution. Q J R Meteorol Soc 139(677):2165–2180. https://doi.org/10.1002/qj.2119

Grams CM, Lang STK, Keller JH (2015) A quantitative assessment of the sensitivity of the downstream midlatitude flow response

to extratropical transition of tropical cyclones. Geophys Res Lett 42(21):9521–9529. https://doi.org/10.1002/2015GL065764
Harr PA, Dea JM (2009) Downstream development associated with the extratropical transition of tropical cyclones over the western North Pacific. Mon Weather Rev 137(4):1295–1319. https://doi.org/10.1175/2008MWR2558.1
Harvey BJ (2016) Human-caused climate change is now a key driver of forest fire activity in the western United States. Proc Natl Acad Sci 113(42):11649–11650. https://doi.org/10.1073/pnas.1612926113
Hersbach H, Bell B, Berrisford P, Hirahara S, Horányi A, Muñoz-Sabater J, Nicolas J, Peubey C, Radu R, Schepers D, Simmons A, Soci C, Abdalla S, Abellan X, Balsamo G, Bechtold P, Biavati G, Bidlot J, Bonavita M, Thépaut J-N (2020) The ERA5 global reanalysis. Q J R Meteorol Soc 146(730):1999–2049. https://doi.org/10.1002/qj.3803
Hodyss D, Hendricks E (2010) The resonant excitation of baroclinic waves by the divergent circulation of recurving tropical cyclones. J Atmos Sci 67(11):3600–3616. https://doi.org/10.1175/2010JAS3459.1
Holden ZA, Swanson A, Luce CH, Jolly WM, Maneta M, Oyler JW, Warren DA, Parsons R, Affleck D (2018) Decreasing fire season precipitation increased recent western US forest wildfire activity. Proc Natl Acad Sci 115(36):E8349–E8357. https://doi.org/10.1073/pnas.1802316115
Jain P, Wang X, Flannigan MD, Jain P, Wang X, Flannigan MD (2017) Trend analysis of fire season length and extreme fire weather in North America between 1979 and 2015. Int J Wildl Fire 26(12):1009–1020. https://doi.org/10.1071/WF17008
Jones SC, Harr PA, Abraham J, Bosart LF, Bowyer PJ, Evans JL, Hanley DE, Hanstrum BN, Hart RE, Lalaurette FO, Sinclair MR, Smith RK, Thorncroft C (2003) The extratropical transition of tropical cyclones: forecast challenges, current understanding, and future directions. Weather Forecast 18:41
Kanamitsu M, Ebisuzaki W, Woollen J, Yang S-K, Hnilo JJ, Fiorino M, Potter GL (2002) NCEP–DOE AMIP-II reanalysis (R-2). Bull Am Meteorol Soc 83(11):1631–1644. https://doi.org/10.1175/BAMS-83-11-1631
Keen RM, Voelker SL, Bentz BJ, Wang S-YS, Ferrell R (2020) Stronger influence of growth rate than severity of drought stress on mortality of large ponderosa pines during the 2012–2015 California drought. Oecologia 194(3):359–370. https://doi.org/10.1007/s00442-020-04771-0
Krawchuk MA, Haire SL, Coop J, Parisien M-A, Whitman E, Chong G, Miller C (2016) Topographic and fire weather controls of fire refugia in forested ecosystems of northwestern North America. Ecosphere 7(12):e01632. https://doi.org/10.1002/ecs2.1632
Molinari J, Knight D, Dickinson M, Vollaro D, Skubis S (1997) Potential vorticity, easterly waves, and eastern pacific tropical cyclogenesis. Mon Weather Rev 125(10):2699–2708. https://doi.org/10.1175/1520-0493(1997)125%3c2699:PVEWAE%3e2.0.CO;2
Orlanski I, Sheldon JP (1995) Stages in the energetics of baroclinic systems. Tellus A 47(5):605–628. https://doi.org/10.1034/j.1600-0870.1995.00108.x
Pantillon F, Chaboureau J-P, Lac C, Mascart P (2013) On the role of a Rossby wave train during the extratropical transition of hurricane Helene (2006). Q J R Meteorol Soc 139(671):370–386. https://doi.org/10.1002/qj.1974
Riboldi J, Grams CM, Riemer M, Archambault HM (2019) A phase locking perspective on Rossby wave amplification and atmospheric blocking downstream of recurving western North Pacific tropical cyclones. Mon Weather Rev 147(2):567–589. https://doi.org/10.1175/MWR-D-18-0271.1
Riemer M, Jones SC (2010) The downstream impact of tropical cyclones on a developing baroclinic wave in idealized scenarios of extratropical transition. Q J R Meteorol Soc 136(648):617–637. https://doi.org/10.1002/qj.605
Schoennagel T, Veblen TT, Kulakowski D, Holz A (2007) Multidecadal climate variability and climate interactions affect subalpine fire occurrence, Western Colorado (USA). Ecology 88(11):2891–2902. https://doi.org/10.1890/06-1860.1
Seager R, Hooks A, Williams AP, Cook B, Nakamura J, Henderson N (2015) Climatology, variability, and trends in the U.S. vapor pressure deficit, an important fire-related meteorological quantity. J Appl Meteorol Climatol 54(6):1121–1141. https://doi.org/10.1175/JAMC-D-14-0321.1
Stuivenvolt Allen J, Wang S-YS, LaPlante MD, Yoon J-H (2021) Three western pacific typhoons strengthened fire weather in the recent northwest U.S. conflagration. Geophys Res Lett 48(3):e2020GL091430. https://doi.org/10.1029/2020GL091430
Vitolo C, Di Giuseppe F, Barnard C, Coughlan R, San-Miguel-Ayanz J, Libertá G, Krzeminski B (2020) ERA5-based global meteorological wildfire danger maps. Sci Data 7(1):Article 1. https://doi.org/10.1038/s41597-020-0554-z
Wagner CEV, Forest P, Station E, Ontario CR, Franais RUE, Davis HJ (1987). Development and structure of the Canadian Forest FireWeather Index System. Canadian Forest Service, forestry technical report
Wallace JM, Zhang Y, Lau K-H (1993) Structure and seasonality of interannual and interdecadal variability of the geopotential height and temperature fields in the northern hemisphere troposphere. J Clim 6(11):2063–2082. https://doi.org/10.1175/1520-0442(1993)006%3c2063:SASOIA%3e2.0.CO;2
Westerling AL (2016) Increasing western US forest wildfire activity: sensitivity to changes in the timing of spring. Philos Trans R Soc B Biol Sci 371(1696):20150178. https://doi.org/10.1098/rstb.2015.0178
Westerling AL, Swetnam TW (2003) Interannual to decadal drought and wildfire in the western United States. EOS Trans Am Geophys Union 84(49):545–555. https://doi.org/10.1029/2003EO490001
Yoon J-H, Kravitz B, Rasch PJ, Wang S-YS, Gillies RR, Hipps L (2015) Extreme fire season in California: a glimpse into the future? Bull Am Meteorol Soc 96(12):S5–S9. https://doi.org/10.1175/BAMS-D-15-00114.1